Book Chapter

Multi-Sensory Opto-Electronic Feature Extraction Neural Associative Retriever

Hua-Kuang Liu and Yahong Jin

Department of Electrical Engineering

University of South Alabama

Mobile, Alabama 36688-0002

Neville I. Marzwell

Jet Propulsion Laboratory

California Institute of Technology

Pasadena, California 91109-8099

and

Shaomin Zhou

Beckman Instruments

Brea, California

December 16., 1996

Abstract

Optical pattern recognition and neural associative memory are important research topics for optical computing. Optical techniques, in particular, those based on holographic principle, are useful for associative memory because of its massive parallelism and high information throughput. The objective of this Chapter is to discuss system issues including the design and fabrication of a multi-sensory opto-electronic feature extraction neural associative retriever (MOFENAR). The innovation of the approach is that images and/or 2-D data vectors from a multiple number of sensors may be used as input via an electrically addressed spatial light modulator (SLM) and hence processing can be accomplished in parallel with high throughput. A set of Fourier transforms of reference inputs can be selectively recorded in the hologram. Unknown image/data can then be applied to the MOFENAR for recognition. When convergence is reached after iterations, the output can either be displayed or used for post-processing computations. We included experimental results that demonstrate the ability of the system to recognize and/or restore input images.

TABLE OF CONTENTS

LIST OF FIGURES

iii

iv

I INTRODUCTION

Optical pattern recognition and neural associative memory are important research areas for optical computing. Optical techniques[1-19], in particular, those based on holographic principle, are useful for associative memory because of its massive parallelism and high information throughput. Some examples include the associative memory systems using four-wave mixing, and self-pumped phase-conjugation in photorefractive crystals and planner holograms. Associative holographic memory has also been proposed via angularly-multiplexed reference beams generated by optical fibers, conventional mirrors and beam splitters. There has been much interest in the possibility of utilizing the advantages of optics to implement various computing architectures that display superior characteristics than those achieved using electronics. Optics offers the potential of more parallel input and processing architectures, and greater flexibility of design for high density interconnect structures.

For the purpose of illustrating the operations of the optical pattern recognition systems, several optoelectronic architectures have been described.

One neural network architecture described in this Chapter is referred to as "MOFENAR", for "Multisensory Opto-electronic Feature Extraction Neural Associative Retriever", utilizes currently available spatial light modulator technology, together with holographic and photorefractive material devices. These elements function together to allow associative memory operation through many parallel channels at once. The network allows the input of data simultaneously from different sensor sources. These data are compared simultaneously, with composite associations being made based upon a previously recorded interconnect hologram located at the Fourier plane. The system capability makes possible the application of the MOFENAR architecture for analysis of many different types of real input signals, either sequentially or simultaneously.

An example of the overall system architecture is represented by the block diagram as shown in Fig. 1. The top part of the Figure shows four CCD Camera and Novelty Sensor Units each of which is receiving input independent of the others. When a new event appearing in the field of view of one of the sensors, the sensor will alert the switching control unit with time and

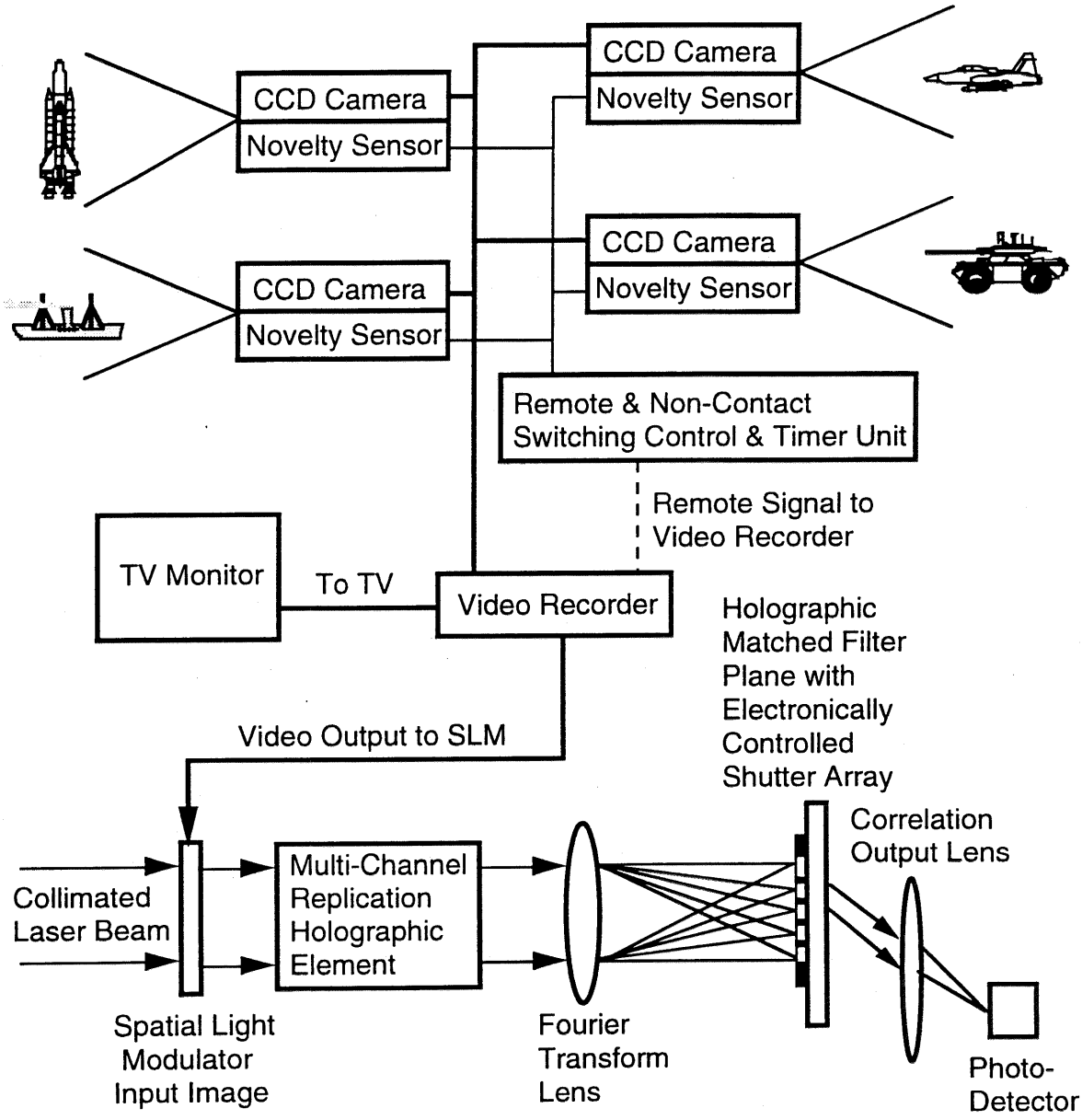

Figure 1 A multi-input multi-channel optical pattern recognition system.

date signal generator. The control unit can remotely control the video recorder for record keeping and displaying of the input signals such as a space shuttle as shown in the upper right corner of the Figure. In the meantime, the input signal is applied to the input ports of an electronically addressed spatial light modulator as shown in the lower part of the system which is redrawn in Fig. 2 and described below.

Figure 2 shows a multi-channel pattern classification system architecture. A laser beam from a HeNe laser is collimated by a spatial filter and lens combination and is then divided into two beams, an object beam and a reference beam. The object beam illuminates the input pattern and is Fourier transformed by the lens at its focal plane where a holographic matched filter is recorded. A multi-channel replication holographic optical element replicates the input into an NxN array of Fourier transforms at the matched filter plane. In the multi-channel pattern classification system the reference beam is angularly multiplexable. During the recording of the matched filter, only one object beam at a time is selected by an electronically controlled shutter array pinhole spatial filter

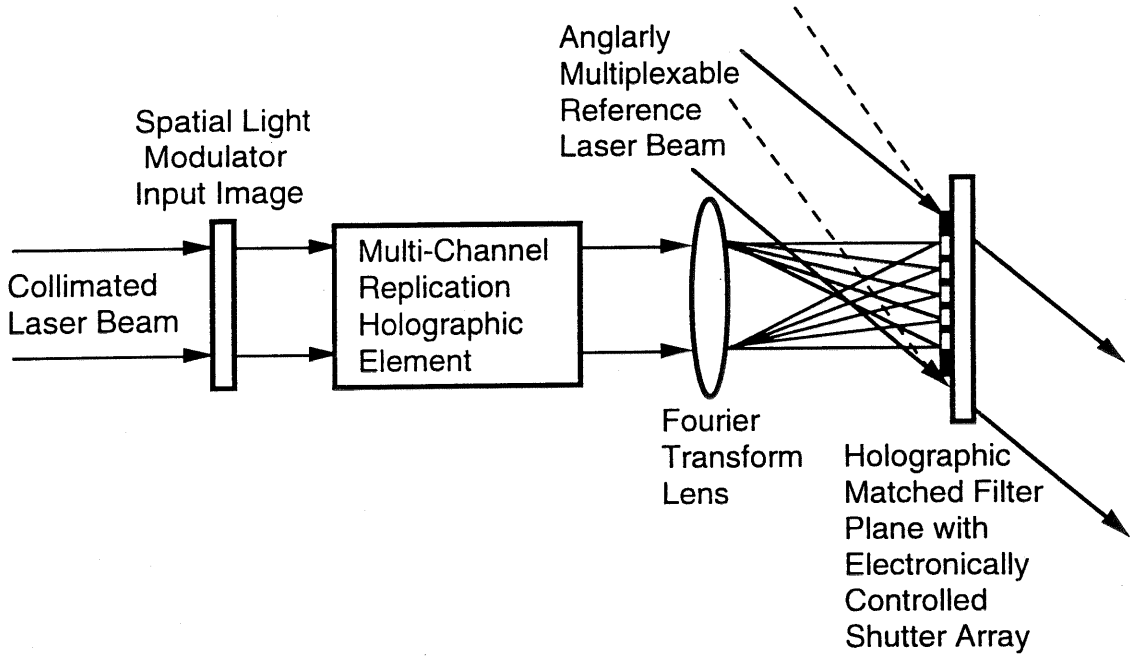

Figure 2 A multi-channel pattern classification system architecture.

and one reference beam angle is used to make the hologram. A different reference beam angle is used to record a different group of objects until all the objects are recorded. The developed hologram becomes the multi-channel matched filter. In the reading process, the matched filter is replaced exactly at its original location and the reference beam is turned off. The signal representing the correlation between the input pattern and the pattern used in the recording of the matched filter can be found at the focal plane of the regenerated reference beam.

These abilities allow the proposed architecture to be applied to many current fields of interest, including parallel database search, image and signal understanding and synthesis, robotic manipulation and locomotion, natural language processing, in addition to real-time multi-channel real pattern recognition.

The MOFENAR architecture is based on iterative optical data array comparisons, and relies upon many principles basic to optical correlation architecture such as the Vander Lugt and the joint Fourier transform. The MOFENAR, however, displays a high-level capability of optically multiplexing each input and comparing this input with many different reference matrices, and creating an oscillatory optical resonance mode in which input variation and error is eliminated in the reconstructed output through a convergent nonlinear optical thresholding process.

In the following, Section II contains a description of a MOFENAR prototype breadboard, including analysis of its operation capability.

Section III describes the specific hardware requirements for the MOFENAR prototype, including optical and electronic components, and both of the input and output data format. Results of neural associative retrieval system's computer simulation are interpreted and conclusions drawn from the simulation are presented. Laboratory experimental results of a single-sensory and multi-sensory optoelectronic feature extraction neural associative retriever are presented to support the theoretical predictions. Section IV is the conclusion.

II SYSTEM DESIGN AND OPERATION

2.1 Experimental System Design

The MOFENAR may be described as a bi-directional feedforward /feedbackward architecture with multi-channel input and processing capability as shown in Figure 3.

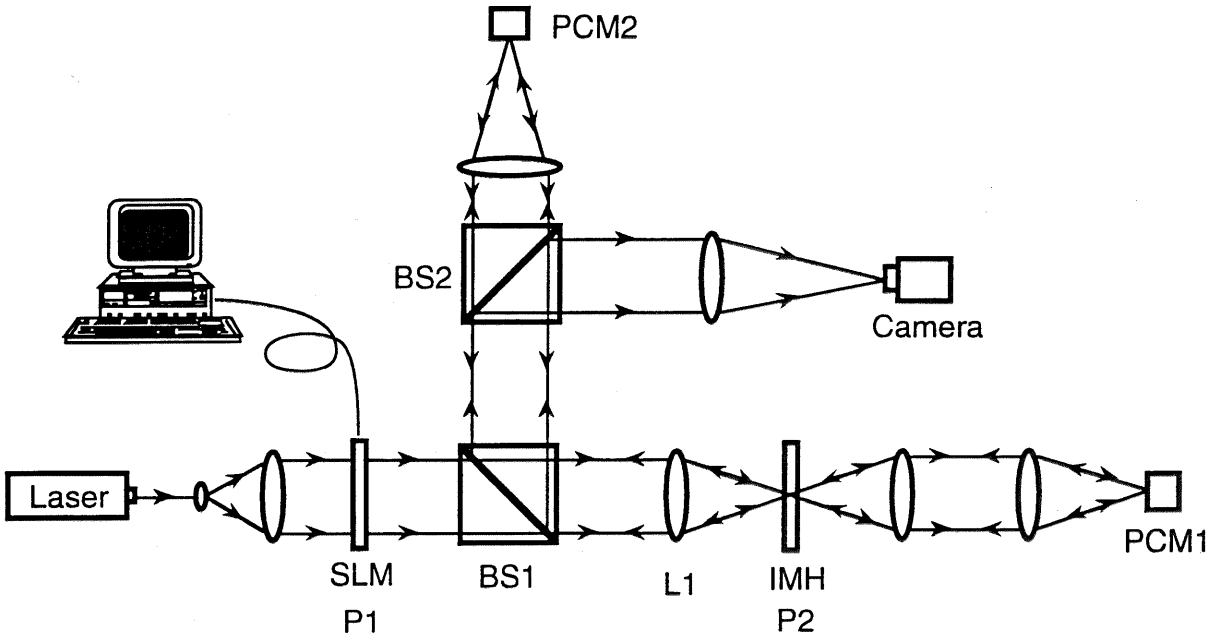

Figure 3 Prototype "MOFENAR" Neural Net Architecture

An expanded, collimated laser beam is used to provide the input to the system. An Argon Ion (514 nm) and frequency-doubled YAG (532 nm) laser are candidates to be selected as the source. The optimal operating wavelength and laser power are to be determined by the characteristics of the specific SLM and PCM obtained for construction of the Phase II prototype design.

The input laser beam is spatially filtered and collimated to the required diameter to optimally couple the laser beam to the input spatial light modulator (SLM).

In the signal processor, the input is arranged in a two dimensional array. This data pattern is then electronically transferred to the SLM. The SLM at plane P1 spatially encodes this pattern onto the input laser beam. The laser beam passes through a beamsplitter (BS1), a Fourier lens (L1), and is focused at the Fourier plane of L1 (P2). BS1 is a polarizing cube beamsplitter placed between the SLM device and L1. This beamsplitter transmits all incident light polarized in one particular orientation, and reflects at ninety degrees all incident light polarized in the orthogonal orientation. This device performs in the same manner regardless of the propagation direction of the incident light.

The "Interconnect Matrix Hologram", (I.M.H.) is placed at the Fourier plane of L1. This hologram consists of a multiplexed array of transmission functions achieved via a translatable mask. This device multiplies the incident focused pattern from the input SLM by its transmission function.

After the focused input pattern passes through and is multiplied by the I.M.H., it is again Fourier transformed by a second single convex lens, L2. At the Fourier plane of this lens, the distribution of light consists of the image of the input patterns recorded in the I.M.H. At this point a photorefractive optical crystal is placed, oriented, and illuminated by two opposing laser beams in such a way as to create a counter-propagation "phase conjugate beam" to each of the incident signal beams. This "phase conjugate mirror" (PCM1) also introduces a nonlinear weighting of reflectivity coefficients, which is dependent upon the intensity of the incident signal beam. This effect results in more intense incident signals being more heavily weighted than less intense signals. If the PCM1 has a natural thresholding effect, then an additional device is not needed. Otherwise, a thresholding device is required (not shown) in front of the PCM1.

The counter-propagation beams generated by PCM1 exactly retrace their incident path through the I.M.H. and onto the polarizing cube beamsplitter. The counter-propagation beam's polarization orientation at this point is orthogonal to the orientation of the original beam. This is

accomplished by correct orientation of PCM1's "pump" beams' polarization, from which the phase conjugate beam is created. Thus, the counter-propagation phase conjugated beams are polarized orthogonally with respect to the input beam, and upon impinging the polarizing cube beamsplitter from the opposite direction, are reflected at ninety degrees. This reflected phase conjugate beam now passes through a second cube beamsplitter, (BS2). This beamsplitter is not a polarizing cube beam splitter like BS1, but is structured such that a constant percentage of incident light is transmitted, and the remainder is reflected, regardless of the incident beam's polarization orientation or direction of propagation. The transmission/reflection ratio may be chosen to be any desired value, and this will be maximized to the largest value possible while still providing sufficient reflected intensity to be recorded by a detector. This small reflected portion is imaged onto a high resolution camera placed one focal length (in optical path length) beyond the second convex lens. The large portion of the phase conjugated beam that is transmitted by the nonpolarizing cube beamsplitter is imaged onto a second PCM (PCM2) also located beyond BS2.

PCM2 is identical in operation to the first, with the exception that the phase conjugate beam which is produced is polarized in the same orientation as the incident beam, unlike PCM1. This is accomplished by orienting the pump beam's polarization orientation parallel to the incident beam's. The counter propagating phase conjugated beam produced by PCM2 retraces the optical path of the incident beam until it is again reflected by PCM1 and reverses its direction. Thus a iterative oscillatory optical wave is created, whose amplitude continuously gains intensity with each pass (assuming the amplification of the PCMs is greater than the losses in a single path) in a manner determined by the nonlinearity of the PCMs' reflectivity until the gain is saturated. At this point a steady state oscillation is established, and a constant output intensity distribution is detected by the camera, giving the neural network's "answer" to the question of the input's information content.

2.2 Experimental System Operation

The architecture described above will demonstrate the associative recall capabilities of the MOFENAR neural net system, along with its fault-tolerance and error correcting capability. Large data storage capacity will be demonstrated in the form of the Interconnect Matrix Hologram.

It can be seen by examining Figure 3 that the two PCMs of the MOFENAR architecture form a partially reflective cavity in which the input beam will oscillate. The simplest example of such oscillation, and how it produces a useful optical output signal, is given here.

If an input pattern or binary vector set is addressed to the input spatial light modulator, and the SLM is illuminated by the input laser, the pattern or vector set will be optically introduced into the MOFENAR system.

The resultant intensity distribution is retro-reflected by the phase conjugate mirror, which can be described as imparting a "time reversal" upon the incident pattern, and thus sending it back the exact same path that it came. Also performed at this point by the nature of the phase conjugation process is a nonlinear thresholding of the optical intensity at plane P3. This thresholding is performed to weigh the most intense parts of the reconstructed image more heavily to remove spurious signals and noise. By more heavily weighting the stronger signals, and "time reversing" the result, the original input image corresponding to these reconstructions will be favored.

The "time reversed" beam created by PCM1 will however not travel back to the original input plane. Because of the intentional orthogonality of the pump beams used to create the phase conjugated, or "time reversed" input beam, this "time reversed" beam is itself polarized orthogonally to the incident beam, and is thus reflected upon its return by the polarizing cube beamsplitter in front of the I.M.H. This beam then travels through an equivalent distance to the plane of the second phase conjugate mirror, PCM2.

At this point, a small constant percentage of the "time reversed" beam has been diverted to the output detector. This output consists of a reconstruction of the input which is more similar to its closest matches within the reference array. By successive iteration through the resonant cavity of the neural net, the output approaches exactly the reference pattern most closely represented by the input.

The major attribute of the neural network is the high rate of information processing that may be achieved. This rate is a function of the degree of parallelism, or number of channels that are implemented, as well as the speed with which the architecture may cycle through successive input patterns.

The two independent elements affecting the system speed are the input spatial light modulator and the phase conjugate mirrors. High resolution spatial light modulators are available which can operate continuously at several hundred frames per second, and operation at over two thousand frames per second has been demonstrated. There is evidence[20-33] indicating that the phase conjugate mirrors will pose a lower limit on system speed than the spatial light modulator, and we therefore examine here the parameters involved in the PCM response time, which is a function of the incident optical intensity, the pump beam optical intensity, and the required reflective gain of the PCM.

We may calculate the optical gain required of the two PCMs by considering the losses involved in a single pass through the neural architecture.

Refer again to Figure 3. By requiring that the power at successive equivalent points in the iterative optical path be equal, we assure a steady optical oscillation, which will converge to the desired output pattern, as described earlier. This analysis allows us to then solve for the required gain of the PCMs, which in turn gives indications of the time required by the PCMs to achieve such gain.

We characterize the individual components' power outputs, or throughputs for the passive components, by using values that are representative of what is currently available:

I_{in} = input laser intensity = 0.1 W/cm^2

I_{PMP} = PCM pump beam intensity = 1.0 W/cm^2

T_{SLM} = input SLM transmission = 0.10

T_{BS1} = beamsplitter 1 transmission = 0.90

T_{IMH} = avg. inter. matrix hologram transm = 0.10

G_{PCM1} = phase conjugate mirror 1 gain = G_1

T_{BS2} = beamsplitter 2 transmission = 0.90

G_{PCM2} = phase conjugate mirror 2 gain = G_2

Using these values, together with the assumption that the IMH multiplexes the input signal into an 11 x 11 array of patterns (see Section 3.1.2), we first find that the optical intensity in one of the recalled images of interest to the right of the IMH in Figure 3

$$\begin{aligned} I &= \frac{I_{in} \times T_{SLM} \times T_{BS1} \times T_{IMH}}{\#\,\text{orders}} \\ &= \frac{100\text{mW} \times 0.1 \times 0.9 \times 0.1}{121} \\ &= 7.44\mu\text{W} \end{aligned} \qquad (1)$$

Following the reconstruction plane of interest through the prototype architecture, and imposing the same intensity value upon the light for the successive passage through the same point of the system (when the light has reflected off of both PCMs one time, and is at the same point just beyond the IMH), we obtain

$$7.44\mu W \times G_{PCM1} \times T_{IMH} \times T_{BS1} \times T_{BS2} \times G_{PCM2} \times T_{BS2} \times T_{BS1} \times T_{IMH} = 7.44\mu W \quad (2)$$

or

$$G_{PCM1} \times T_{IMH} \times T_{BS1} \times T_{BS2} \times G_{PCM2} \times T_{BS2} \times T_{BS1} \times T_{IMH} = G_{PCM1} \times 0.1 \times 0.9 \times 0.9 \times G_{PCM2} \times 0.9 \times 0.9 \times 0.1 = 1 \quad (3)$$

which requires that

$$(G_{PCM1})(G_{PCM2}) = 152 \quad (4)$$

Thus to overcome the losses in each iterative path through the neural net architecture, a combined gain of 152 is required. This gain may be split between the two PCMs, and the factorization will be determined by the available intensity at each PCM along with the associated response time to achieve the required total gain.

This is as far as a quantitative temporal analysis of the MOFENAR performance can practically go, for the following reasons. Photorefractive four wave mixing (the basis of phase conjugation) is a physical process which achieves a steady state optical condition when the input signal is applied constantly. The investigations that have been reported in the literature into the response of photorefractive crystals have for the most part concentrated on this steady state operation, where reflective gains of up to 100 have been reported. For the "MOFENAR" neural net architecture, we are instead concerned with the response of the photorefractive elements when presented with pulses of short duration, on the order of or less than the "response time" of the material itself.

III HARDWARE CONSIDERATION AND EXPERIMENTAL DEMONSTRATIONS

The proposed MOFENAR architecture consists of currently available opto-electronic devices and device technology components combined to achieve high speed pattern recognition and optical signal processing. The hardware elements available today are described, and the system integration and software design requirements are discussed in the following section.

3.1 Hardware Considerations

As presented earlier, an important aspect of the proposed architecture is that it calls for largely available devices and device technology to construct a breadboard prototype system. The major elements of the system include the spatial light modulator, multifocus Fourier transform architecture, interconnect matrix hologram, and photorefractive phase conjugate mirrors to be used at the ends of the iterative optical cavity. A discussion of the current performance capability and availability of each follows.

3.1.1 Spatial Light Modulator

The input data to the "MOFENAR" technology originates at one or more sensors measuring the field of interest. The signals from these sensors must be incorporated onto the input light beam. This is accomplished through the use of an addressable spatial light modulator.

Such a device transfers an input optical or electronic signal onto a coherent collimated beam of light, in most cases a laser. Optically addressed devices include the Hughes Liquid Crystal Light Valve (LCLV). Electrically addressed devices include the Magneto-Optic SLM (MOSLM), the STC Ferroelectric Liquid Crystal SLM (FLCSLM), the liquid crystal television(LCTV) SLM, and the Texas Instruments Deformable Mirror Device (DMD). The areas which can be used to quickly determine the apparent device of choice are speed and availability. The liquid crystal devices are

currently capable of no more than 100 frames/second. The higher speed devices are the Texas Instruments DMD and the MOSLM. We select the MOSLM as an example for the purpose of discussion.

The MOSLM device has also been shown to be more robust a device than any of the liquid crystal SLMs. Results of successful military shock and vibration tests performed upon the 128x128 array, as well as its documented wide temperature range of operation were recently presented.

Table 3.1 gives specifications of MOSLM and STC FLMSLM for comparison. The MOSLM outperforms the STC device not only in speed, but also is available in higher resolution, and achieves much higher contrast. The STC ferroelectric SLM demonstrates greater transmission and wavelength flexibility.

Table 3.1 Characteristics of two available 2-D spatial light modulators.

Performance Category	**MOSLM**	**STC FLMSLM**
Resolution	48^2,128^2,256^2	128^2
Contrast Ratio	>10,000:1	>100:1
Transmission	>14%	>65%
Wavelength Range	514 to 850 nm	0.5 to > 1 nm
Frame Rate	>1000 f/s	>100 f/s

The MOSLM device consists of an array of individually addressable pixels. These pixels may be switched to two oppositely magnetized homogeneous states, as well as to a heterogeneously magnetized state, referred to as the "neutral" magnetization state. The pixels operate by rotating the plane of polarization of incident light clockwise or counterclockwise, depending upon which of the two homogeneous magnetic states the pixel is switched to. When an incident linearly polarized beam is transmitted through the device, the output polarization is rotated

clockwise or counterclockwise in a manner dictated by the pixels switched states. This polarization modulation is translated to an amplitude or phase modulation by placing an analyzer polarizer in the path of the transmitted beam. When the polarizer's transmission axis is oriented perpendicular to one of the two output polarization angles, the light passing through pixels switched to that state is extinguished, while that passing through pixels switched to the opposite homogeneous state is partially transmitted. This modulation is referred to as "binary amplitude only" modulation, and is shown below in Figure 4.

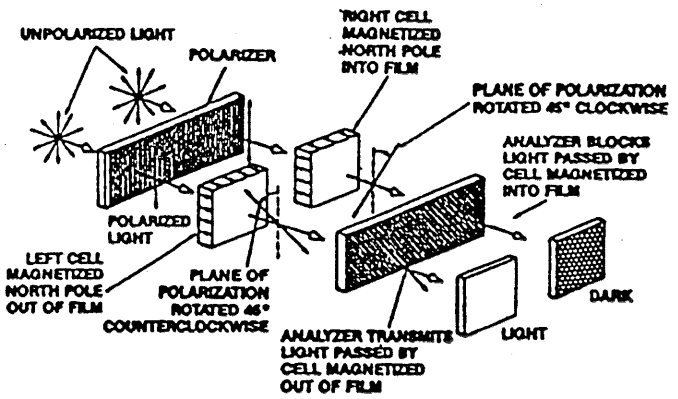

Figure 4 Principle of Operation of the MOSLM.

If alternatively, the analyzer polarizer's transmission axis is oriented perpendicular to the bisector of the two output polarization angles, the transmitted amplitude is the same for all pixels, but the phase of light from pixels switched in one homogeneous state is 180 degrees out of phase with that of the light from pixels switched in the opposite homogeneous magnetization state. This modulation is referred to as "binary phase only" modulation. For non binary operations, liquid crystal devices with lower speed need be considered.

3.1.2 Multifocus Fourier Transform Device

To accomplish the desired replication of the input pattern's two dimensional Fourier transform, the inherent structure of the MOSLM spatial light modulator may be utilized. However,

to achieve intensity uniformity throughout the replication plane, an alternative holographic solution would consist of custom manufacturing a single hologram that would be placed after the input MOSLM, and which would result in the required uniform replication of the Fourier transformed input pattern.

Figure 5 shows an example of a Fourier replication due to pixelation of an input function. The computer simulation program used to demonstrate this feature assumes a fixed focal length, and thus only shows a fixed portion of the replicated field, but in fact the replication period may be adjusted at will by varying the Fourier lens.

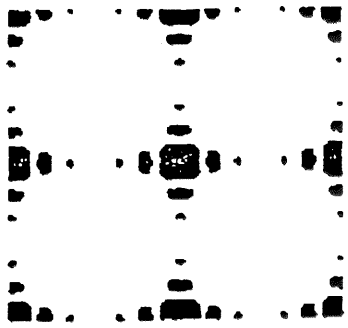

Figure 5 Example of Fourier Pattern Replication Due To Input SLM pixel array.

The MOSLM, as well as other similar devices, contains opaque rows and columns between the rows and columns of active pixels. This becomes a two dimensional grating when the MOSLM is used in a Fourier system, such as here, and the result is a replication at the Fourier plane of whatever image is programmed onto the MOSLM. The spacing of the replications depends upon the focal length of the Fourier transforming lens, the spacing of the pixels in the MOSLM, and the incident wavelength. Thus by choosing the focal length of the Fourier lens, we achieve a two dimensional periodic replication of the desired Fourier transform pattern.

The intensity of the replicated Fourier transforms falls off with increasing order. This falloff was experimentally measured using a 128^2 MOSLM array and an incident 633 nm. laser beam, and values are given in Table 3.2, along with the required recording time for each to cancel

the intensity variation. If one assumes that the efficiency of the recorded hologram is proportional to the recording time, then by inverting the intensity value of each order, and using that number as a relative recording time, the net transmission will be a constant.

Thus the IMH hologram recorded using these first 5 orders of the MOSLM would require a recording time up to 100 times longer for the outer orders than for the strongest zero order replicated pattern.

Table 3.2 Experimental 128^2 array replicated output intensities, and calculated corrective recording times.

Order	Measured Intensity	Recording Time
0	47.5 μW	1.00 T(0)
+1	27.3	1.74
-1	35.5	1.34
+2	3.00	15.8
-2	7.95	6.00
+3	1.40	33.9
-3	2.00	23.8
+4	0.45	105.
-4	0.90	52.8
+5	0.85	55.9
-5	2.30	20.7

Binary optic gratings are another applicable technology which potentially could be used to complement the effect of the SLM grating itself, making the replication intensity more uniform.

3.1.3 Interconnect Matrix Hologram (I.M.H.)

This element, placed at the Fourier plane of the MOFENAR architecture, must enact the required phase and amplitude modulation upon the incident optical beam to satisfy the learning rules which are to be implemented within the MOFENAR system. This element must also display high resolution recording capability in order to enact the desired transmission function at each of the locations of the replicated optical Fourier transform incident from the input MOSLM. The device will be encoded in the following manner.

Refer to Figure 6. A desired reference data pattern, a(x,y) + b(x,y), is first encoded on the spatial light modulator, which in turn encodes the pattern onto the laser beam. This pattern is then optically Fourier transformed and replicated, as discussed above.

An aperture is placed just in front of the I.M.H., equal in size to a single replicated Fourier pattern, and centered over one of the replicated order locations. A holographic recording is then made of the joint Fourier transform intensity pattern. Note that only the section of the I.M.H. illuminated by the aperture is recorded.

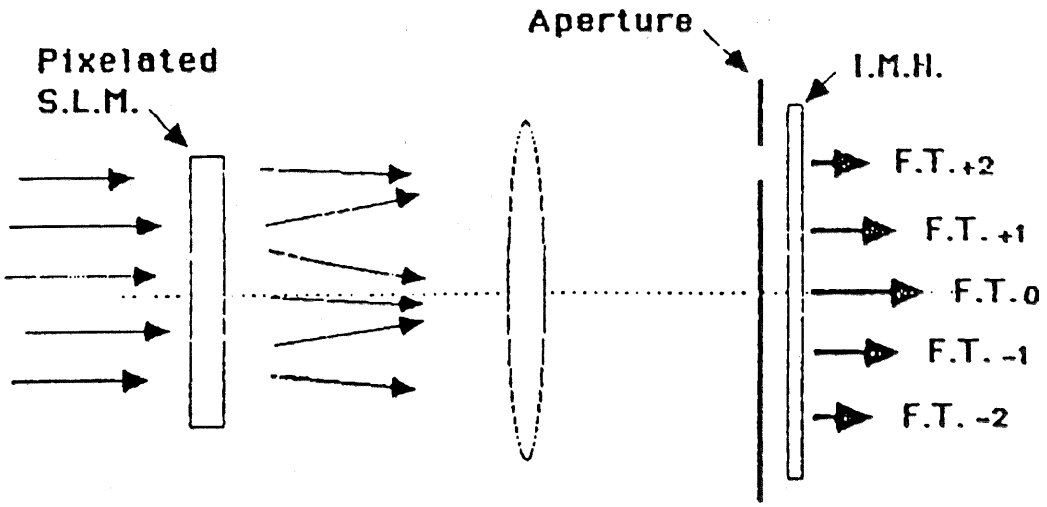

Figure 6 Interconnect Matrix Hologram Recording Process

After recording one Fourier hologram in the I.M.H., the input laser is blocked, the input MOSLM is reprogrammed with a different desired pattern (either a(x,y), b(x,y) or both are changed), and the aperture is translated to an adjacent location on the I.M.H. This process is repeated throughout the plane of the I.M.H., until a complete array of reference holograms is achieved in the I.M.H.

The recording time is varied to correct for the incident intensity variation. By using a recording time that is inversely proportional to the intensity of the particular replicated order, the efficiency of the I.M.H. may be altered to cancel this variation and produce equivalent outputs for any of the recorded orders. Table 3.2 presents calculated recording times for the case of the 128x128 MOSLM array.

Noting the dramatic fall off in intensity for the device in going from the zero order to the plus and minus fifth orders, this seems a reasonable limit of replications to attempt in a prototype MOFENAR architecture. This results in 121 different reference data patterns being stored in the I.M.H. When these data patterns have been recorded, the aperture is removed.

Because the non uniformity of the diffraction pattern may cause a problem in the reading of the hologram and in the amplification, reflection, and thresholding operations, it may be necessary that an H.O.E. be utilized to achieve a more uniform replication. The drawback here is the reduction of light throughput, as limited by the HOE's diffraction efficiency.

3.1.4 Phase Conjugate Mirrors

Another, perhaps most challenging element of the proposed breadboard prototype are the phase conjugate mirrors (PCMs). These devices produce a phase conjugated, opposing beam to that which is incident upon the surface of the mirror. Such a beam exactly retraces the path of the incident beam, and therefore may be described as a "time reversed" equivalent to the incident

beam. It is this "time reversal" of the incident wave that makes possible the iterative optical processing of the input pattern.

The architecture that has been studied over the last several years to accomplish phase conjugation is known as "four wave mixing", and is shown in Figure 7.

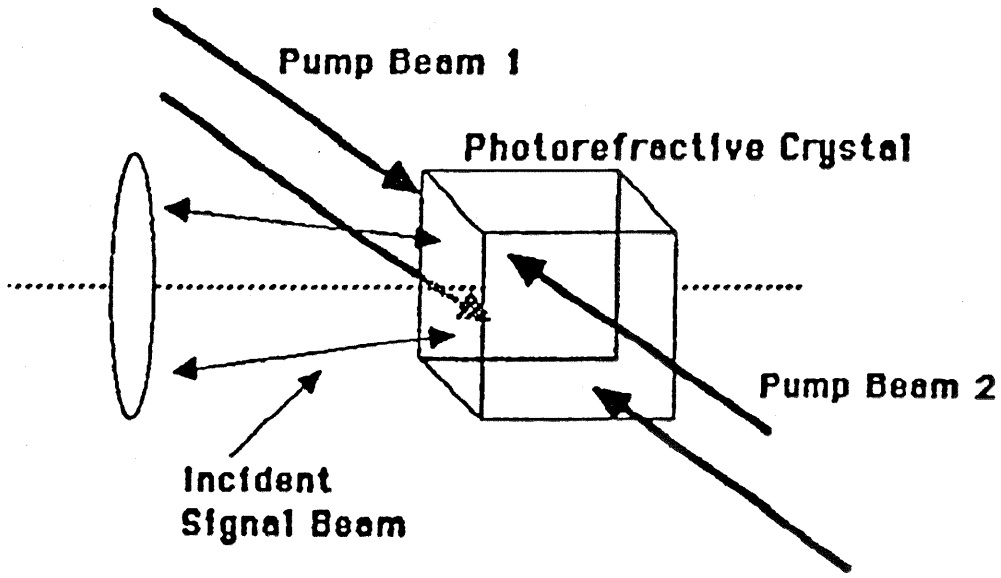

Figure 7 Phase conjugate mirror architecture.

Interference of the incident signal beam and a plane wave pump beam 1 forms an intensity pattern in the crystal. This intensity distribution creates a charge migration in the photorefractive crystal that results in a corresponding refractive index change. Pump beam 2, also a plane wave, enters the crystal from the opposite direction as pump beam 1, and is diffracted by the index modulation. The result of this diffraction is the creation of a phase conjugated beam counter propagating along the path of the incident signal beam. If the intensity of pump beam 2 is much greater than that of the signal beam, the diffracted intensity of the phase conjugated beam may exceed that of the incident signal beam, and gain is achieved. This gain is simply a result of coupling between the incident and plane wave beams. Such amplification has been previously shown in $BaTiO_3$.

Here we present some specific points regarding the performance and characteristics of four photorefractive materials used in four wave mixing experiments:

$LiNbO_3$ is a well studied material, and is perhaps more available than others. It has a small electro-optic coefficient, fast response time, small diffraction efficiency. The response time increases for smaller grating periods, while sensitivity (gain) increases with period. Sensitivity is low due to small carrier drift and diffusion lengths.

$BaTiO_3$ has a large electro-optic coefficient, and relatively slow response times (100 ms for approximate 100 mW/cm^2 intensity). Its response time decreases for smaller grating periods. Its gain increases for smaller grating periods, and for less intense signal beams. Amplified phase conjugation has been demonstrated in $BaTiO_3$, and this material is capable of very good performance under correct conditions.

BSO has a small electro-optic coefficient, poor sensitivity, and fast response time. It is strongly optically active, and poorly understood (e.g., input-output polarization relationship, transmitted-diffracted beam interaction, polarization states).

SBN is another material that is not well documented. It has been suggested that it can be made to perform[21] comparably to $BaTiO_3$. It has a slow response time (sec. with $1W/cm^2$ intensity).

In general, for all of the above materials the steady state gain saturates for large pump/input beam intensity ratios ($I_{pump}/I_{input} >> 1$). As this ratio gets smaller, e. g., less than 1000, the gain decreases.

Two requirements of the PCM for the MOFENAR application include the ability to achieve gain between the incident and reflected phase conjugate beam, as well as the ability to perform nonlinear optical thresholding upon the incident intensity distribution. The first requirement is necessary due to attenuating effects present elsewhere within the cavity, namely losses due to

absorption and scattering. The second requirement exists to achieve the desired self correcting, adaptive capability described above.

A third requirement of the PCM is that it respond at least as quickly as the input pattern cycles. This is seen by recalling above that it is the incident beam itself which forms the grating within the PCM that creates the phase conjugate beam. Therefore every time the input changes, and thus the incident beam distribution changes, the desired grating in the PCM must be reformed before the new incident beam will be phase conjugated.

Finally, an important aspect of this element of the MOFENAR architecture is the availability of photorefractive crystals. An investigation into availability led to the conclusion that there are in fact few sources available to those interested in simply purchasing crystals to experiment with. Much of the research that has been performed in this area has been done by those who have the capability to grow such devices themselves (or whom are directly associated with those who can grow the devices). There are devices available however, and one centimeter cube single crystals of both $BaTiO_3$ and BSO can be obtained within a reasonable amount of time.

3.2 Experimental Demonstrations

There are many examples of the applications of optical pattern recognition techniques[34-52]. In this section, we present two optical pattern recognition experiments to demonstrate the feasibility of the MOFENAR. First we discuss the input/out format to the system.

The input to the MOFENAR architecture consists of electrical signals from one or more detectors, which are fed to the input MOSLM. The formatting of these signals requires standard, consistent mapping onto the MOSLM for efficient associative recall to be achieved. To accomplish this input data formatting for the SLM, software may be written which processes the individual signals from each of the utilized detectors. Frame grabbers are available for the acquisition, digitization, and processing of input images and signals. Real images may also be processed by the

MOFENAR architecture. Examples of real image input and multi-sensor input architecture that are feasible with the neural net are shown in Figures 8a and 8b.

The output of the MOFENAR architecture consists of the reconstructed reference pattern which is found by the iterative optical neural network algorithm implemented in the MOFENAR system. This output may be read directly in the case of real image analysis and pattern recognition, or may be analyzed with a dedicated electronic state circuitry custom tailored to the specific application in which the MOFENAR is utilized.

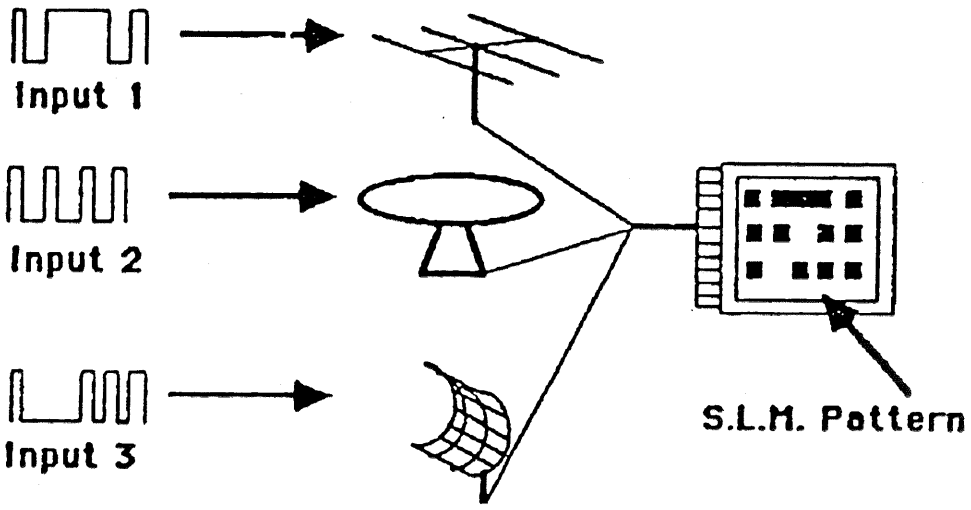

Figure 8a Real Image Input to the MOFENAR neural net.

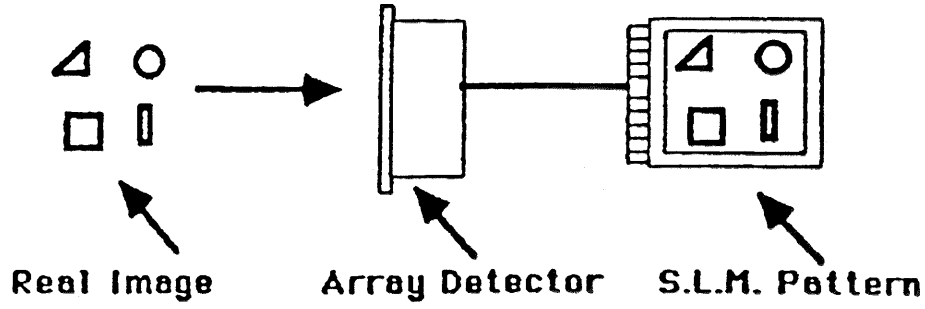

Figure 8b One or Multi-Sensor MOFENAR Input Architecture.

The optically generated output of the MOFENAR may also be analyzed optically, using standard optical processing architecture such as the Vander Lugt correlator or a digital optical signal processing network.

First, the experimental demonstration of an architecture of single-sensory opto-electronic feature extraction neural associative retriever (SOFENAR) is accomplished. Then, a MOFENAR with electronic feedback and angularly/or spatially multiplexed is demonstrated.

3.2.1 Single-sensory Opto-electronic Feature Extraction Neural Associative Retriever (SOFENAR)

First, we discuss two kinds of SOFENARs with optical feedback and electronic feedback, respectively. The experimental demonstration for the scheme with optical feedback is presented.

a. SOFENAR with Optical Feed-back

An optical feedback SOFENAR is shown in Fig. 9. In the recording (memorizing) step, the shutter is turned on, and the object beam carrying complete input information passes through a Fourier transform lens (FL), interfers with a reference beam to write a dynamic grating in a holographic medium. The grating includes three components, $|O|^2 + |r|^2$, Or^* and O^*r, where O represents the Fourier transform of the object o, r denotes the reference beam, and symbol "*" means phase conjugation. In the retrieval step, the shutter is turned off, the object beam carrying incomplete input information (o') to readout the hologram to generate a part of the related reference beam (r'), the reference beam is counter-propagated by using a mirror (M) to readout the same hologram again, so that the corresponding complete object, $\mathbf{F}\{(O' O^*)|r|^2 O^*\}$, can be obtained from output plane via a beam splitter (BS), where O' means the Fourier transform of the incomplete input object o' and **F** represents Fourier transform operation. In this scheme, the holographic medium can be either planner or volume materials.

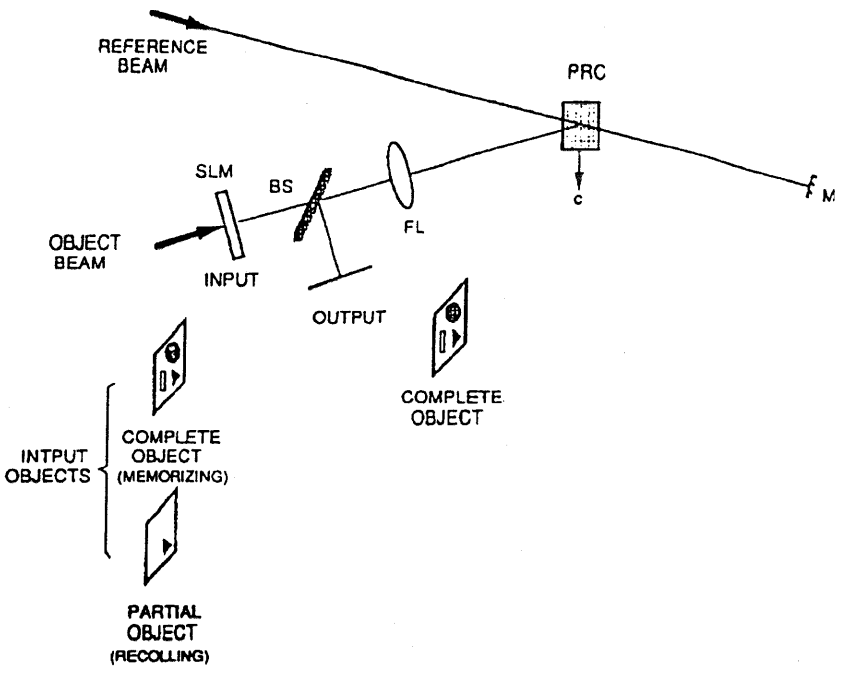

Figure 9 Optical feedback SOFENAR by using volume holographic medium and conventional mirror.

Figure 10 shows experimental results of 2-D image associative sensing by using the optical feedback SOFENAR, Two images are shown respectively in (a) and (b). Left part and right part represent an incomplete input object and a completely reconstructed complete object, respectively. The reversed reconstructed-objects in vertical direction is come from the reverse imaging of the optical setup.

In addition to the images shown in Figure 9, the image of a finger print is used to demonstrate the feasibility of the system. Results are shown in Figs. 11-15. An Air Force resolution chart is used to show the resolution of the system in the retrieved image. Results are shown in Figs. 16-18. From these results, we may conclude that when the diameter of the aperture of the image is 1/5, only incomplete retrieval can be obtained. When the diameter is increased to

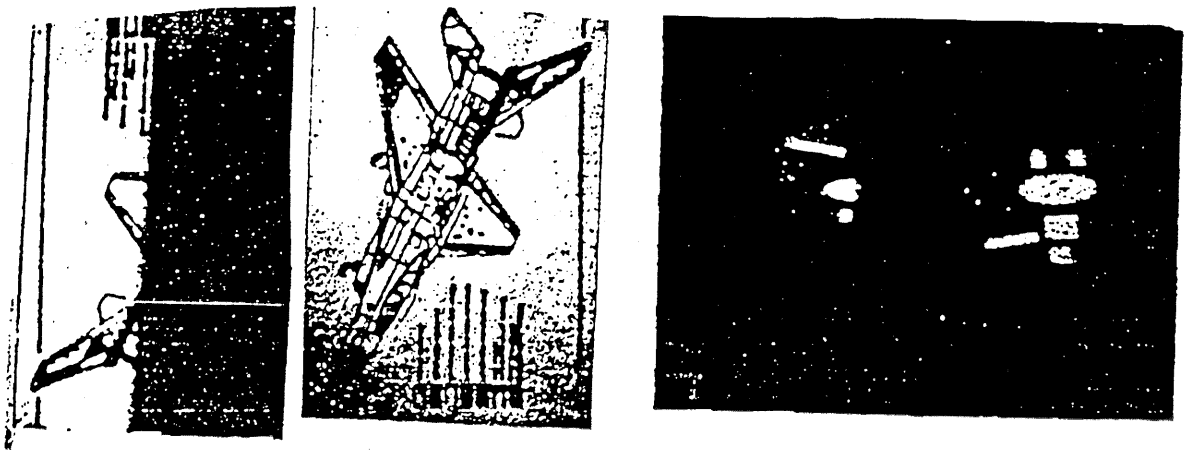

Figure 10 Experimental results. (a) Image object 1, and (b) Image object 2. The left part and the right part are the incomplete input objects and reconstructed complete objects, respectively.

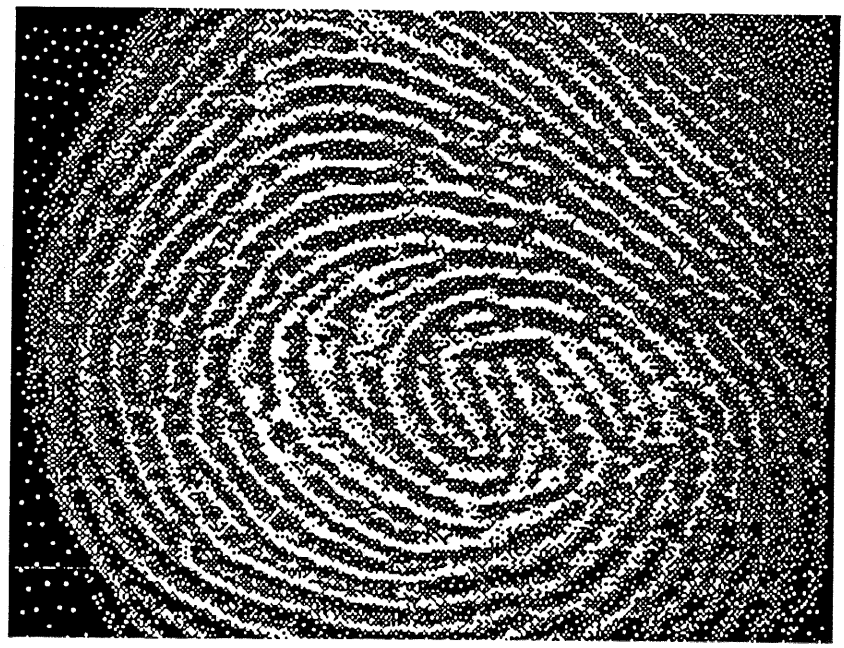

Figure 11 The original image of a finger print stored in a PC and reproduced from a laser printer.

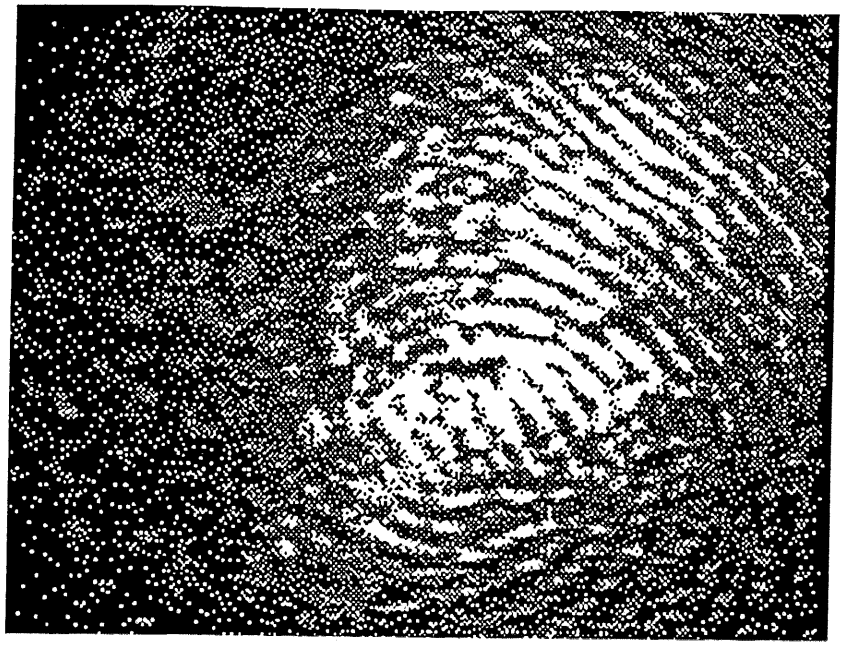

Figure 12 The retrieved image of the finger print with an original input that is limited by an aperture of 1/5 of the diameter centered at the image.

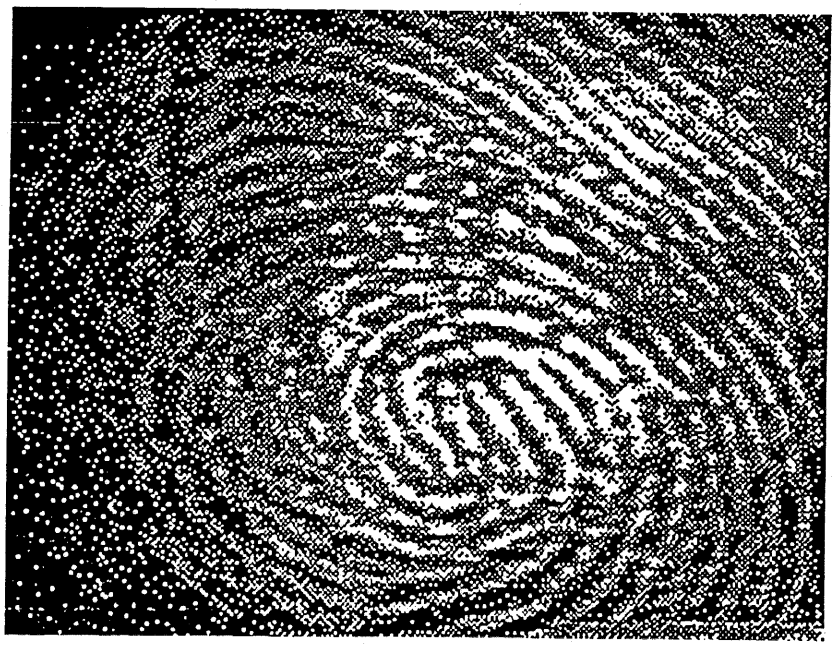

Figure 13 The retrieved image of the finger print with an original input that is limited by an aperture of 1/2 of the diameter centered at the image.

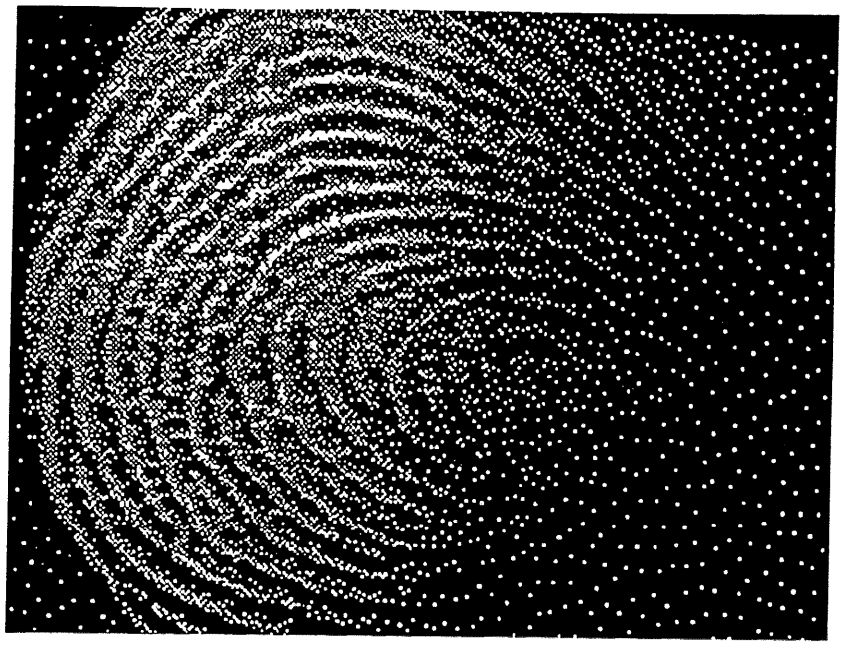

Figure 14 The retrieved image of the finger print with an original input with its right half blocked.

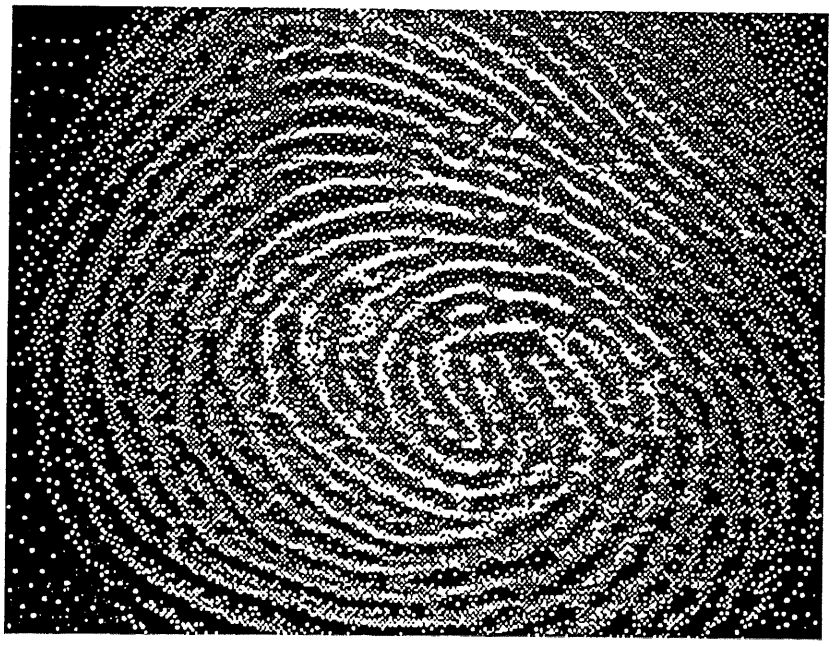

Figure 15 The retrieved image of the finger print with an original input with its left half blocked.

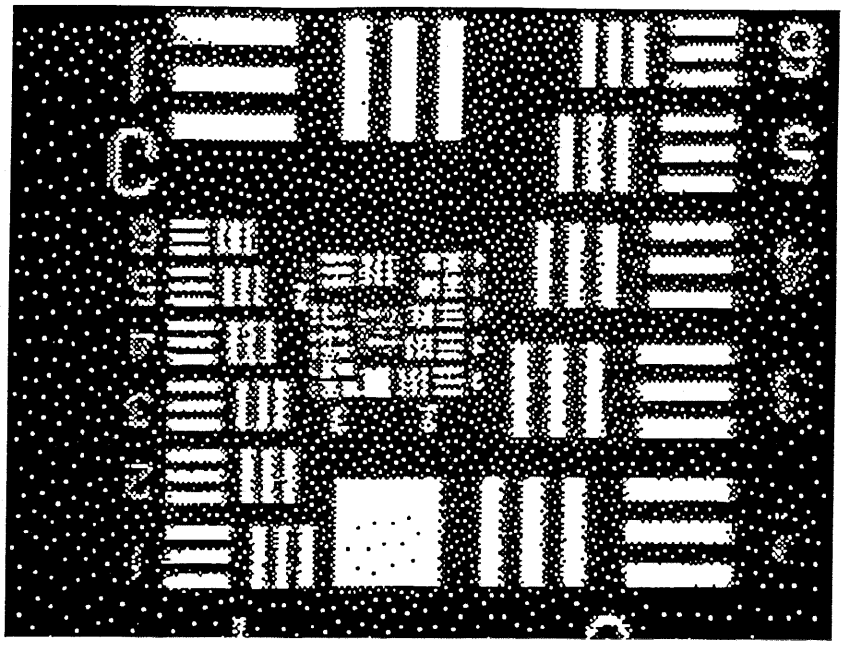

Figure 16 The original image of an Air Force resolution chart stored in a PC and reproduced from a laser printer.

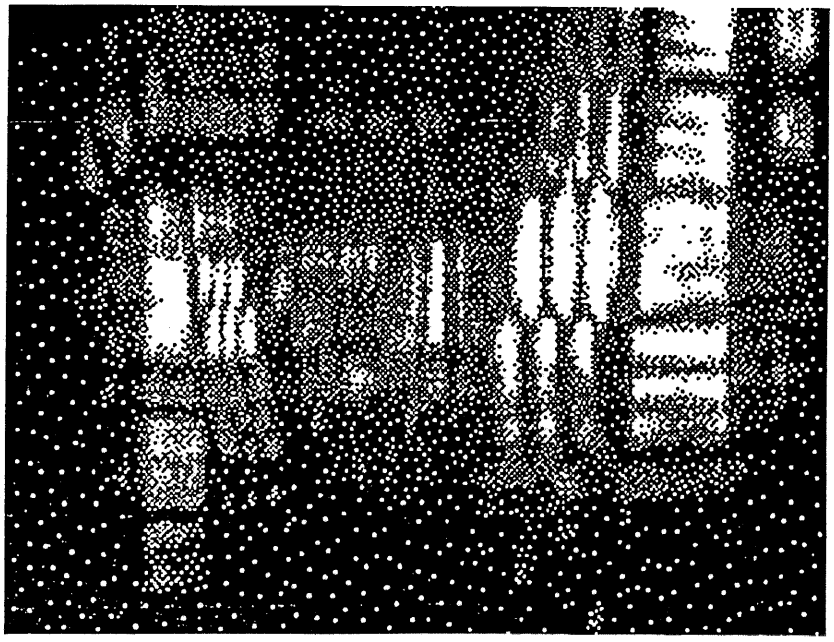

Figure 17 The retrieved image of the resolution chart with an original input that is limited by an aperture of 1/5 of the diameter centered at the image.

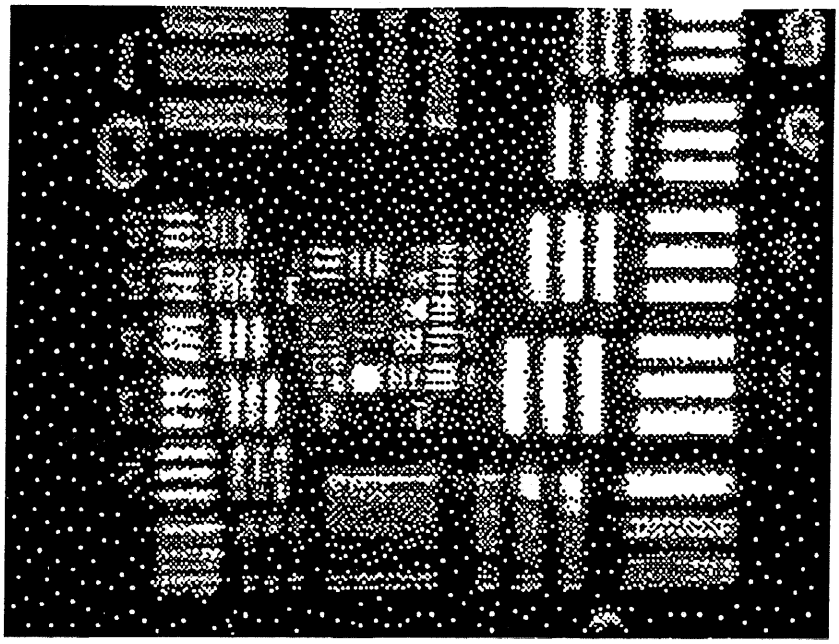

Figure 18 The retrieved image of the resolution chart with an original input that is limited by an aperture of 1/2 of the diameter centered at the image.

1/2, reasonable retrieval is obtainable. Also, the image retrieval process is asymmetrical in the horizontal direction due to the thick volume recording property of the photorefractive crystal.

b. Electronic feedback SOFENAR

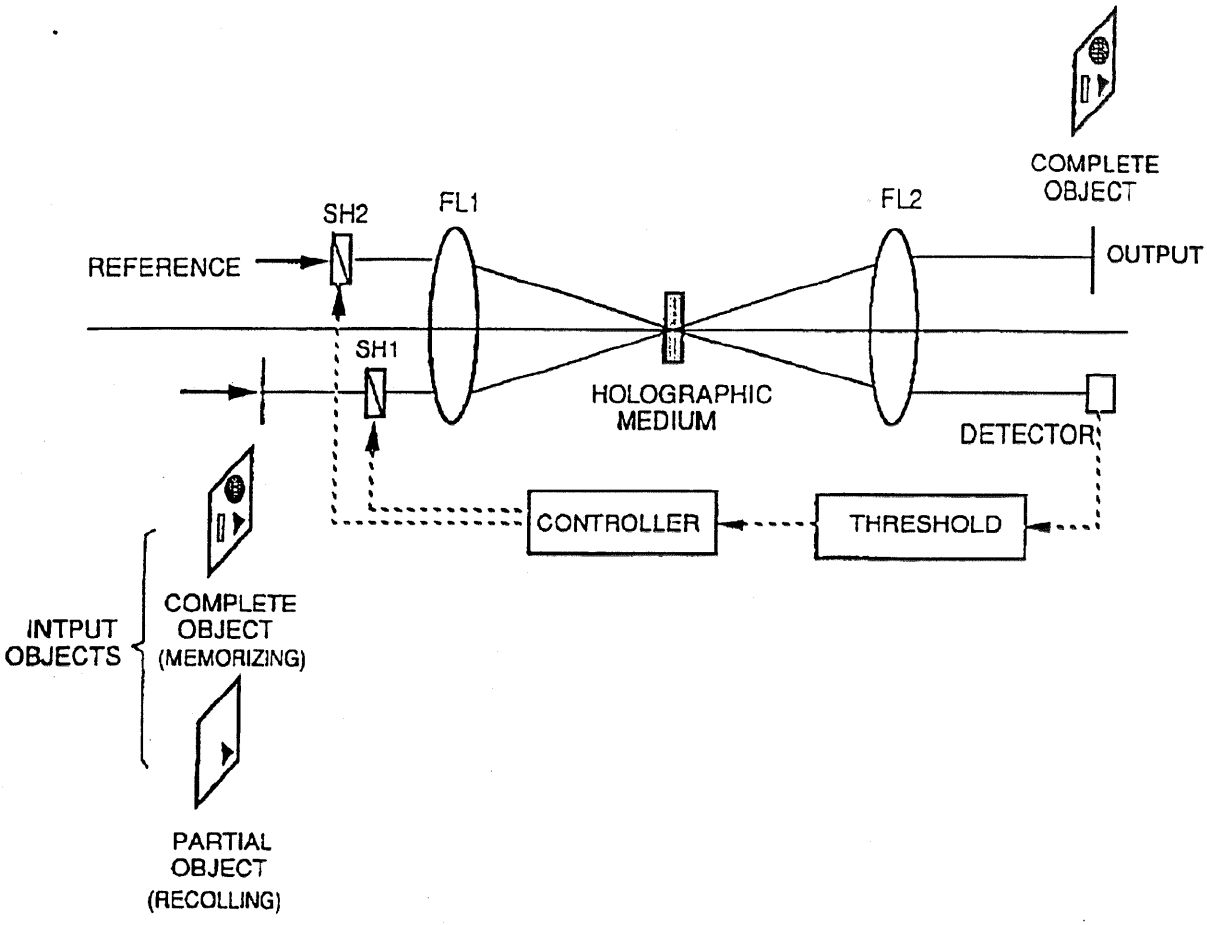

Figure 19 Electronic feedback SOFENAR. The holographic medium is either a thick volume or a thin planner material.

The electronic feedback SOFENAR is shown in Fig. 19. In the memorizing step, both shutter 1 and shutter 2 are turned on, and the interference grating is recorded with a holographic medium passing through FL1. In the sensing step, shutter 1 is turned off and shutter 2 is turned on at beginning, the incomplete input object generate a partial reference beam and incident into a detector. The electronic signal output from the detector passes though a thresholding device and a controller to reverse the states of these two shutters as long as the intensity of the reconstructed reference beam is large than a certain value set in advance. The original reference beam passes through the shutter 1 to readout the complete object from output plane via FL2.

The SOFENARs described above can be expanded to become a MOFENAR by using angularly and/or spatially multiplexed recording with either optical and/or electronic feedback arrays. We first present the architecture of electronic feedback MOFENAR with angular multiplexing and spatial multiplexing and then show an experimental feasibility demonstration.

3.2.2 Multi-Sensory Opto-Electronic Feature Extraction Neural Associative Retriever (MOFENAR)

a. Electronic feedback angularly-multiplexed MOFENAR

The architecture of the optical feedback SOFENAR (see Fig. 9) may be modified to form a MOFENAR by using angularly multiplexed reference beam in a volume holographic medium, as shown in Fig. 20. An N x M (1 x 3 in the Fig. 20) Dammann grating (DG) is used to generate a N x M angularly multiplexed replicates of an incident plane-wave reference. Lenses L2 and L3 are used to image the rear surface of the DG to a photorefractive crystal (PRC). The passage of each angularly multiplexed reference beam in the array can be individually controlled by using a

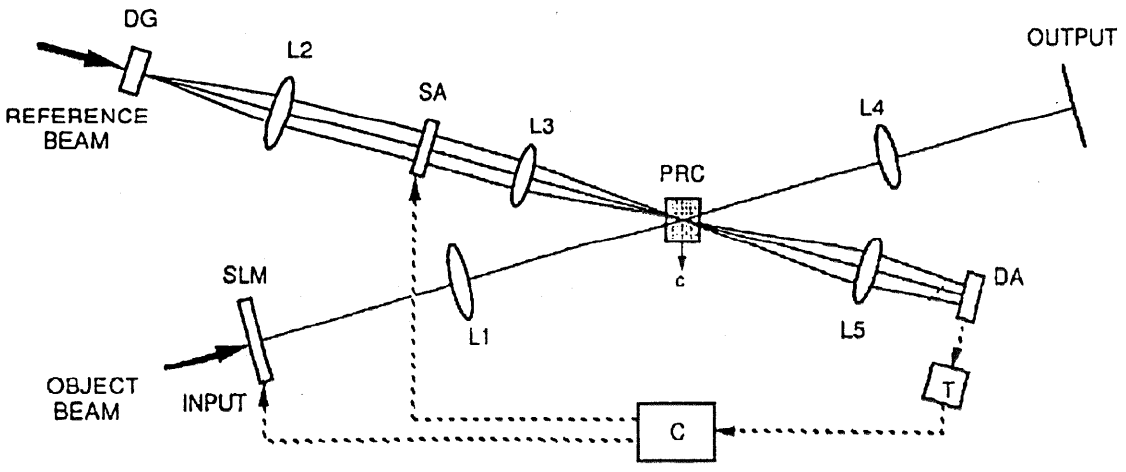

Figure 20 Angularly multiplexed MOFENAR with an electronic feedback, a photorefractive crystal, and a Dammann grating.

corresponding shutter array (SA), which is located on the focal plane of L2. In the recording step, step, a series of inputs from a spatial light modulator (SLM) are Fourier transformed with lens L1 and recorded on the PRC with different reference beam by controlling the SA. In the retrieval step, all elements of the SA are turned off, and an incomplete object input from the SLM is Fourier transformed and used to readout a part of the related reference beam which is then focused by lens L5 and detected with a certain element of the detector array (DA). The electronic signal output from the detector element is then used to control the SA and SLM(after removing the incomplete input object from the SLM and turning on the corresponding element of the SA) via the threshold device and the controller. The specific reference beam passing through the SA and generate a complete object out of the incomplete input object. This output is obtained at the image plane of lens L4.

b. Electronic feedback spatially-multiplexed MOFENAR

b.1 *Architecture*

An electronic feedback spatially-multiplexed MOFENAR can be constructed by using a spatially-multiplexed reference beams in a planner holographic medium, as shown in Fig. 21. In this architecture, the configuration of the reference beam is the same as that of the previous Figure. A Dammann grating (DG2) is used to generate an N x M spatially-multiplexed replications of the Fourier transform of the input object. A shutter array (SA2) is used to individually control the propagation state (passing or blocking) of each replicated beam, and only one replicate at one time is allowed to address the holographic medium. If one input is recorded at one location of the hologram, then N x M different inputs may be recorded(e.g., N=M=3 in Fig. 21). At the beginning of the retrieval, SA2 is turned on and SA1 is turned off. The partial reference beam generated by the related incomplete input is then detected, thresholded, and used to turn off SA2 and turn on the element of SA1 to readout the corresponding complete image.

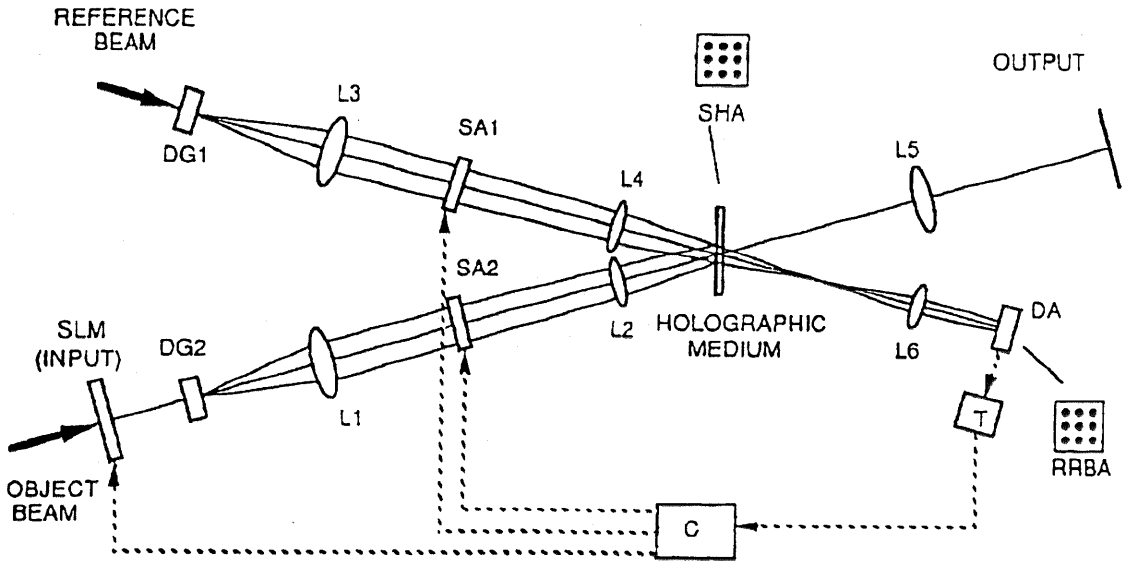

Figure 21 Spatially-multiplexed MOFENAR with an electronic feedback, a planner holographic medium, and two Dammann gratings.

b.2 *Experimental Results*

The experimental set-up of a three-channel electronic-feedback MOFENAR are shown in Figs. 21 and 22. Attention is called to Fig. 22. The laser beam comes from the 514.5 nm line of a Coherent Innova 306 Ar^{+3} laser which passed through a half-wave plate (HP1), and is splitted by a polarizing beam splitter (PBS) into two; an ordinary beam and an extraordinary beam. The transmitted extraordinary beam is expanded, spatially-filtered, and collimated using lens L1, a pin-hole spatial filter, and lens L2. This is the object beam. A double Mach-Zehnder interferometer is used to provide three input paths for inputs of A, B, and C. Three shutters SH1-SH3 can be used to select the specific input for recording and recalling. The input object beam is then Fourier transformed by lens L3 and applied to a photorefractive crystal (PRC). The reflected ordinary beam from the PBS is converted to an extraordinary beam using a half-wave plate (HP2) which then illuminates a 1 x 3 optical fan-out element (OFE) and generates three reference beams with equal intensities. The transmission of the three reference beams are controlled by three shutters(SH4-SH6). During learning, the six shutters are turned on a pair at a time(SH1 and SH4,

SH2 and SH5, SH3 and SH6) to record three individual complete input objects via angular multiplexing in the PRC. At the beginning of the retrieval process, shutters SH4-SH6 are turned off, and one of the shutters SH1-SH3 (e.g., SH1) is turned on to apply an incomplete object (e.g., A) to reconstruct the corresponding reference beam and unavoidably also due to cross-talk some other reference beams. These reference beams are sensed by a photo-detector array D1 with a proper threshold for the suppressing of the cross-talk terms. The correctly associated reference beam which is selected after thresholding is then feedback to turn on the corresponding shutter (e.g. SH4) to reconstruct the complete image of the object (e.g. A) through lens L5 and detector array D2.

In the experiment, the objects chosen are three different space shuttle images (i.e. DISCOVERY, ATLANTIS, and COLUMBIA). Figure 23 shows the three reconstructed reference beams when the three incomplete objects are applied. Figures 24-26 show three sets of

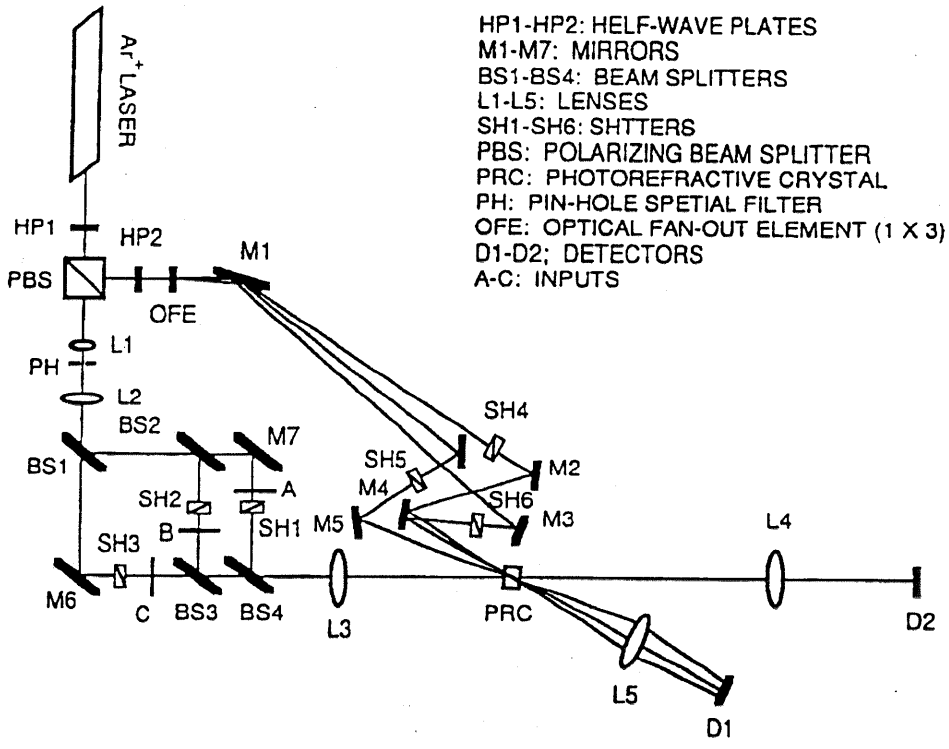

Figure 22 The experimental set-up of a MOFENAR with electronic feedback .

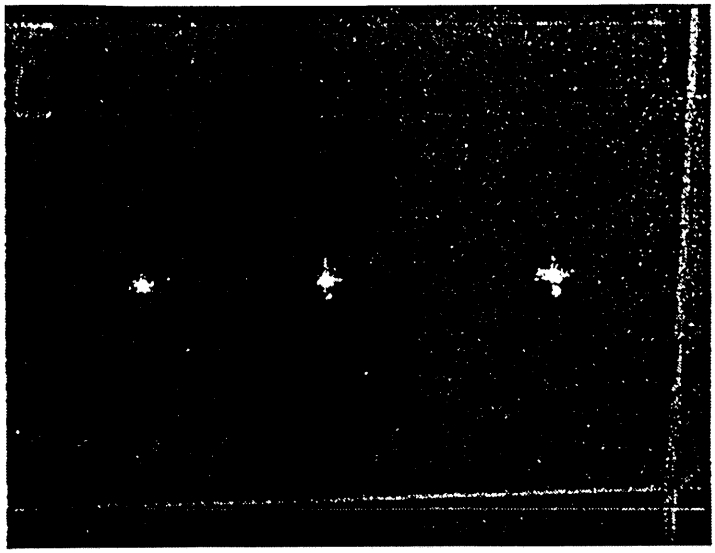

Figure 23 The three reference beams reconstructed by three complete inputs corresponding respectively to the image of space shuttle DISCOVERY(left spot); ATLANTIS(middle spot); and COLUMBIA(right spot).

associatively retrieved images. In each of the Figures, (a) shows the incomplete input object; (b), the reconstructed reference beam; and (c), the retrieved complete object.

IV Conclusions

We have presented the results of a thorough theoretical and experimental investigation on the characteristics and capabilities of a novel optical neural network pattern recognition architecture. We have presented detailed analyses and experimental results and have constructed experimental systems utilizing state-of-the-art optical elements and devices which are either currently available or can be obtained in a reasonable time and manner.

The major elements of this investigation include the theoretical design and explanation of the proposed system architecture and operation, a computer simulation investigation into the implementation of desired learning rules and performance of the system in various applications, and an investigation of the hardware elements required for the implementation of the breadboard system.

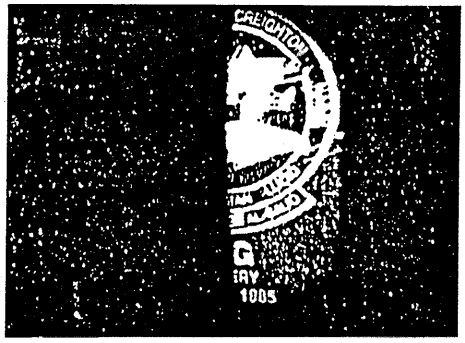

(a)

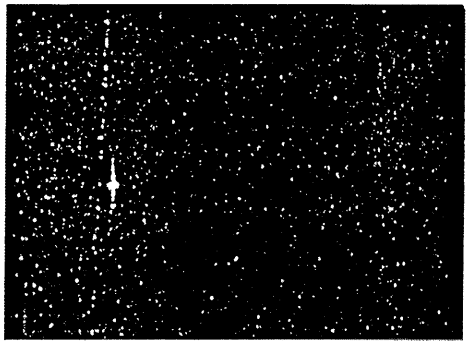

(b)

(c)

Figure 24 Associative retrieval experiment; input with DISCOVERY.(a) Incomplete input, (b) reconstructed reference, and (c) retrieved.

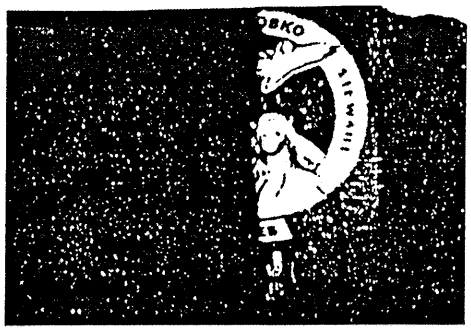

(a)

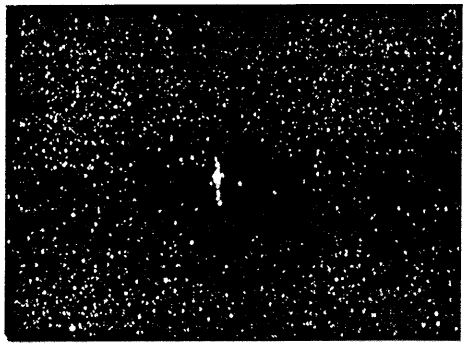

(b)

(c)

Figure 25 Associative retrieval experiment; input with ATLANTIS. (a) Incomplete input, (b) reconstructed reference, and (c) retrieved.

(a)

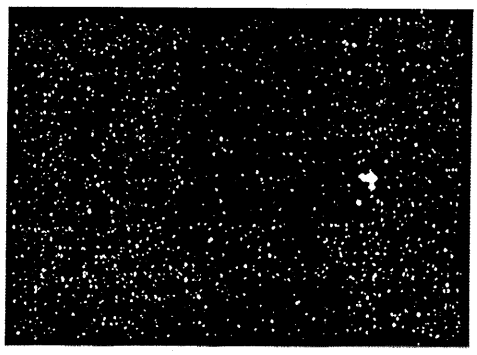

(b)

(c)

Figure 26 Associative retrieval experiment; input with COLUMBIA. (a) Incomplete input, (b) reconstructed reference, and (c) retrieved.

The individual elements required for implementation of such a system are currently available. A spatial light modulator which is currently capable of demonstrating frame rates of over 1000 per second has been documented, and standard dichromated gelatin holographic technology is shown to allow the resolution necessary for a prototype implementation such as is proposed. The phase conjugate mirrors show great promise, and experimental application of various crystals as phase conjugate mirrors is investigated and referenced. However, the body of experimental data on this new field of optics is as yet not sufficient for a definite conclusion to be drawn on the exact performance of such materials in the proposed MOFENAR system. Some important questions regarding these materials are raised in the following section.

A mathematical model of the MOFENAR principle of operation was derived. This formalism was subsequently translated to computer code form, and implemented to provide simulation results of the performance of such a system. These results were documented and presented, which support the conclusion that the MOFENAR system does indeed offer the capability of adaptive, fault tolerant operation.

Using both angularly multiplexed and spatially multiplexed MOFENAR described above, a large number (an order of thousands) of objects may be memorized and sensed, in parallel. The designed MOFENAR with electronic feedback is of large information capacity, good discrimination capability, and high image quality.

As shown above, the MOFENAR architecture offers significant potential capability to perform parallel multi-sensory recognition of input patterns or vector sets originating from multiple sensors, which measure either identical or different types of signals. This capability has direct potential applications in several fields, including parallel database search, image and signal understanding and synthesis, and robotics manipulation and locomotion, in addition to real-time multi-channel real pattern recognition.

In the following sections, we examine some of the possible applications that may utilize the capability of the MOFENAR neural net, and indicate how they might be investigated using the proposed prototype system.

4.1 Real Images

The most obvious application of the MOFENAR architecture is a neural pattern recognition tool, for use in NASA and/or industrial environments. The input patterns may be directly fed to a spatial light modulator from a standard or nonstandard video camera. This input may be one of a known set of potential inputs. The set of known potential inputs may be stored in matrix form in the Interconnect Matrix Hologram. Thus, the input pattern, which may contain noise or variations, will create a closest "match" with the most similar stored reference image, and the thresholding, iterative optical processing of the MOFENAR will distinguish and recreate this reference pattern at the output plane of the neural network. This output may either be presented for direct visual confirmation, or may be used as an input into an optical post processor, such as a standard optical correlator.

One example of such a utilization of the MOFENAR is robotics vision. The proposed neural network offers the capability of a relatively compact optical processing system to handle imperfect visual input and draw conclusions based upon its own reference library of patterns. This may allow real-time vision analysis to be performed, which could be translated to independent robotics locomotion and environmental interaction.

4.2 Related Vector Sets

The second major area in which the MOFENAR neural network might be well utilized is in the processing of large and complex data sets, either from a single detector or source, or from more than one detector simultaneously.

Known data patterns which are to be searched for may first be encoded in the Interconnect Matrix Hologram of the architecture, as described in Section 4.1. The input SLM may then be fed continuous information from detectors aimed at the field(s) of interest, and the MOFENAR architecture will in parallel compare each input frame with all of the stored reference data patterns in the IMH. Any input data frame which contains a pattern sufficiently similar to one of those stored in the IMH will result in the ideal reconstruction of only that pattern at the output plane of the neural network.

Not only does this allow for direct large scale compares and recognition of data to be accomplished in parallel, but it also presents the capability of inferring information from the input, and establishing new recognition rules to be sought and found. This is due to the fact that each input pattern will result in some output that indicates how the input data pattern compares and is similar or dissimilar to, the data patterns stored in the IMH. Thus one may attempt to "teach" the neural network to recognize any and all levels of data patterns present in the incoming signals, both on the level of the discrete data itself and on higher levels of data field. Documentation of the "MOFENAR" output in a training mode may allow the repeated ability to infer information from the input of previously unusable or unseen data patterns.

One specific application is a common problem which currently requires massive electronic computing capability. This is weather condition analysis. Individual sensors measuring humidity, temperature, wind velocity, and pressure for example, at one or several locations, and representing a single time or a set of consecutive temporally separated measurements, may be translated to spatial binary representation, relayed to the input spatial light modulator of the MOFENAR, and processed. The Interconnect Matrix Hologram in this case could consist of experimentally recorded data from the same sensors, which is known to precede specific weather patterns or conditions. The output from the MOFENAR in this case may be evaluated on different levels as described above, and statistical or empirical relationships between the output weather condition vector set and the actual measured weather condition may be drawn.

In summary, a few potential NASA and commercial applications are summarized below:

NASA Applications

a) Planetary exploration in-situ data analysis and information screening

b) Space surveillance specific object identification and navigation guidance

c) Space image understanding and classification

d) Space station automated rendezvous and docking

e) Space habitation and utilization environmental evaluation and assessment

f) Navigation collision avoidance in Moon and Mars

g) Satellite repair, maintenance and sensing

Commercial applications

a) Criminal finger prints random access memory and retrieval for police

b) Security check commercial building entrances

c) Automobile plate identification

d) Large capacity free space interconnection for future computers

e) Border patrol and illegal drug traffic prevention

ACKNOWLEDGEMENT

The authors would like to acknowledge the support of the research work by the Jet Propulsion Laboratory, California Institute of Technology, under contract with the National Aeronautical and

Space Administration. The work of Standard International Corporation, and Professor Pochi Yeh of the University of California at Santa Barbara was funded under a NASA- SBIR contract No. NAS7-1307.

V BIBLIOGRAPHY

(1) H. C. Longuet-Higgins, *Nature*, **217**, 104 (1968).

(2) D. Gabor, *IBM J. Res. Devel.*, **13**, 156 (1969).

(3) D. Psaltis and N. Farhat, in *ICO-13 Conf. Digest* (International Commission for Optics, Amsterdam, 1984), paper A1-9.

(4) A. D. Fisher and C. L. Giles, in *Proc. of IEEE*, Compcon Spring (Institute of Electrical and Electronics Engineers, New York, 1985), 342 (1985).

(5) G. J. Dunning, E. Marom, Y. Owechko, and B. H. Soffer, *J. OSA.* **A2 (13)**, 48 (1985).

(6) H. J. Caulfield, *Opt. Commun.* **55**, 80 (1985).

(7) H. Mada, *Appl. Opt.* **24**, 2063 (1985).

(8) S. Y. Kung and H. K. Liu, *SPIE Proc.*, **613**, 214 (1986).

(9) H. K. Liu, S. Y. Kung, and J. Davis, *Opt. Eng.*, **25**, 853 (1986).

(10) B. H. Soffer, G. J. Dunning, Y. Owechko, and E. Marom, *Opt. Lett.*, **11**, 118 (1986).

(11) Y. Owechko and B. H. Soffer, *Opt. Lett.*, **16**, 675 (1991).

(12) A. Yariv, S. K. Kwong, and K. Kyuma, *Appl. Phys. Lett.*, **48**, 1114 (1986).

(13) O. Changsuk and P. Hankyu, *SPIE Proc.*, **963**, 554 (1988).

(14) H. Yoshinaga, K. Kitayama, and H. Oguri, *Opt. Lett.*, **16**, 669 (1991).

(15) J. W. Goodman, "*Introduction to Fourier Optics*", McGraw Hill, NEW YORK, 1968.

(16) D. Z. Anderson, D. M. Lininger, M. J. O'Callahan, "Competitive Learning, Unlearning, and Forgetting in Optical Resonators," *IEEE Proceedings*, Conf. on Neural Information Processing Systems-Natural and Synthetic (1987).

(17) Y. Z. Liang, D. Zhao, and H. K. Liu, "Multifocus Dichromated Gelatin Hololens," *Appl. Opt.*, 22, p2351 (1983).

(18) J. Davis and J. Waas, "Current Status of the Magneto-Optic Spatial Light Modulator", *SPIE O-E Lase 89*, San Diego.

(19) J. Waas and M. Waring, "*Spatial Light Modulators; A User's Guide*", The Photonics Design and Applications Handbook 1989", Teddi C. Laurin, Pittsfield, MA (1989).

(20) Y. Fainman, E. Klancnik and S. Lee, "Optimal Coherent Image Amplification by Two-Wave Coupling in Photorefractive BaTiO3", *Opt. Eng.*, **25**(2) (1986).

(21) G. Valley and M. Klein, "Optimal Properties of Photorefractive Materials for Optical Data Processing", *Opt. Eng.*, **22**(6) (1983).

(22) G. Rakuljic, R. Ratnakar, et.al., "Self-Starting Passive Phase Conjugate Mirror with Ce-Doped Strontium Barium Niobate", *App. Phys. Lett.*, **50**(1) (1987).

(23) G. Gheen and L. Cheng, "Optical Correlators with Fast Updating Speed Using Photorefractive Semiconductor Materials", *App. Opt.*, **27**(3) (1988).

(24) P. Yeh, et.al., "Photorefractive Nonlinear Optics and Optical Computing", *Opt. Eng.*, **28**(4) (1989).

(25) F. Laeri, T. Tschudi and J. Albers, "Coherent CW Image Amplifier and Oscillator Using Two-Wave Interaction in a BaTiO3 Crystal", *Opt. Comm.*, **47**(6) (1983).

(26) J. Fienberg, et.al., "Photorefractive Effects and Light-Induced Charge Migration in Barium Titanate", *J. App. Phys.*, **51**(3) (1980).

(27) D. Ledoux and J. Huignard, "Two-Wave Mixing and Energy Transfer in $BaTiO_3$ Application to Laser Beamsteering", *Opt. Comm.*, **49**(4) (1984).

(28) V. Vinetskii, et. al., "Dynamic Self-Diffraction of Coherent Light Beams", *Sov. Phys. Usp.*, **22**(9) (1979).

(29) A. Marrakchi and J. Huignard, "Diffraction Efficiency and Energy Transfer in Two-Wave Mixing Experiments with $Bi_{12}SiO_{20}$ Crystals", *App. Phys.*, **24** (1981).

(30) H. Rajbenbach, J. Huignard, B. Loiseaux, "Spatial Frequency Dependence of the Energy Transfer in Two-Wave Mixing Experiments With BSO Crystals", *Opt. Comm.*, **48**(4) (1983).

(31) B. Fischer, et.al., "Amplified Reflection, Transmission, and Self-Oscillation in Real-Time Holography", *Opt. Lett.*, **6**(11), (1981).

(32) J. P. Huignard and A. Marrakchi, "Coherent Signal beam Amplification in Two-Wave Mixing Experiments with Photorefractive $Bi_{12}SiO_{20}$ Crystals", *Opt. Comm.*, **38**(4) (1981).

(33) A. Yariv, "Phase Conjugate Optics and Real-Time Holography", *IEEE J. Quantum Electron.*, **QE-14**, 650-660 (1978).

(34) A. Vander Lugt, "The effects of small displacements of spatial filters," *Appl. Opt.*, **6**(7), 1221-1225 (1967).

(35) D. Casasent and A. Farman, "Sources of correlation degradation," *Appl. Opt.*, **16**(6), 1652-1661 (1977).

(36) A. Shimizu and M. Hase, "Entry method of fingerprint image using prism," *Trans. Inst. Electronic Comm. Engineers Japan*, Part D, **J67D**(5), 627 (1984).

(37) L. Cai, S. Zhou, P. Yeh, Y. Jin, N. Marzwell and H. K. Liu, "Translation sensitivity adjustable compact optical correlator and its application for fingerprint recognition", *Opt. Eng.*, **35**, 415 (1996)

(38) A. B. Vander Lugt, "Signal detection by complex spatial filtering," *IEEE Trans. Inf. Theory*, **IT-10,** 139-145 (1964).

(39) V. V. Horvath, J. M. Holeman and C. Q. Lemmond, "Holographic technique recognizes fingerprints," *Laser Focus* , **6**, 18-23 (1967).

(40) F. T. Gambe, L. M. Frye, and D. R. Grieser, "Real-time fingerprint verification system," *Appl. Opt.*, **31**, 652-655 (1992).

(41) C. S. Weaver and J. W. Goodman, "A technique for optically convolving two functions," *Appl. Opt.*, **5**, 1248 (1966).

(42) K. H. Fielding, J. L. Horner and C. K. Makekau, "Optical fingerprint identification by binary joint transform correlation," *Opt. Eng.*, **30**(12), 1958-1961 (1991).

(43) J. Ohta, J. Sharpe, and K. Johnson, "An optoelectronic smart detector array for the classification of fingerprints," *Opt. Commun.*, **111**, 451-458 (1994).

(44) Zikuan Chen, Ying Sun, Yanxin Zhang, and Guoguang Mu, "Hybrid optical/digital access control using fingerprint identification," *Opt. Eng.*, **34**(3), 834--839 (1995).

(45) A. Vander Lugt, "Practical considerations for the use of spatial carrier-frequency filters," *Appl . Opt.*, **5**(11), 1760-1765 (1966).

(46) L. Sadovnik, A. Rizkin, O. Rashkovskiy and A. A. Sawchuk, "All-optical invariant target recognition based on intensity-to-phase coding", *Opt. Eng.*, **35**, 423 (1996)

(47) X. J. Lu, C. Y. Wrigley and D. A. Gregory, "Basic parameters for miniature optical correlators employing spatial light modulators", *Opt. Eng.*, **35**, 429 (1996)

(48) R. Burzynski, M. K. Casstevens, Y. Zhang and S. Ghosal, "Novel optical components: second-order nonlinear optical and polymeric photorefractive materials for optical information storage and processing applications", *Opt. Eng.*, **35**, 443 (1996)

(49) X. Yang and Z. H. Gu, "Three-dimensional optical data storage and retrieval system based on phase-code and space multiplexing", *Opt. Eng.*, **35**, 452 (1996)

(50) M. Montes-Usategui, J. Compos, J. Sallent and I. Juvells, "Complex sidelobe removal by a multichannel procedure", *Opt. Eng.*, **35**, 514 (1996)

(51) A. Gonzalez-Marcos and J. A. Martin-Pereda, "Digital Chaotic output from an optically processing element", *Opt. Eng.*, **35**, 525 (1996)

(52) P. Blonda, V. la Forgia, G. Pasquariello and G. Satalino, "Feature extraction and pattern classification of remote sensing data by a modular neural system", *Opt. Eng.*, **35**, 536 (1996)

CLEARANCE NO. 27

PREPUBLICATION REVIEW RECORD

INSTRUCTION: Check statement of circumstances applicable to this clearance and indicate action taken.

APPLICABLE CIRCUMSTANCE(S):

1. (X) A JPL "reportable item" is not disclosed but may exist or be "in the making." (NOTE: Originate Notice of New Technology).

2. ( ) JPL or ( ) JPL SubK unreported "reportable item" is disclosed. (NOTE: Originate Notice of New Technology - if SubK, request NTR and decline clearance until NTR is received. Caltech and NMO to review for foreign filing when "item" is within a statutory class of patentable subject matter).

3. ( ) Reported item of new technology is disclosed - U.S. Patent Application filed. (NOTE: Look for reportable and/or patentable improvements. Ask NMO or Caltech for instructions if any are found).

4. ( ) Reported item of new technology is disclosed - no U.S. Application filed. (NOTE: Look for new reportable subject matter for new NTR. If subject matter for new NTR is present, it should be prepared. If a patent application has been ordered or is in preparation, the new subject matter should be brought to the attention of the attorney as soon as possible and foreign filing review by Caltech and NMO is essential.

5. ( ) JPL SubK invention, of other 3rd party invention, will be disclosed. (NOTE: Deny clearance unless written permission to publish has been obtained from invention owner).

ACTION TAKEN:

( ) Talked with _____ Tel. ____
( ) Reviewed: ( ) abstract ( ) manuscript ( ) title of publication only.

( ) Notice of New Technology originated - copy of clearance, abstract, manuscript or article put in case folder.

( ) Because this is not a JPL invention, written permission of invention owner for JPL publication has been confirmed.

( ) Foreign filing Review. Clearance approved by:

R. E. Jones 1/17/97
NMO Rep. Date

J. Rooney/CIT 1-15-97
~~CIT Rep.~~ Date

CLEARANCE: ( ) Recommended (✓) Conditional - see Comments ( ) Delayed - see Comments

COMMENTS:

PREPARED BY: